



Linking atmospheric and urban auralization models

Philipp Schäfer* , Lennart Reich, and Michael Vorländer

Institute for Hearing Technology and Acoustics, RWTH Aachen University, Kopernikusstraße 5, 52074 Aachen, Germany

Received 26 January 2022, Accepted 8 June 2022

Abstract – In a recent publication, we presented an efficient method to find eigenrays in a stratified, moving medium. The simulation framework is designed to auralize aircraft flyovers. However, the method is restricted to the direct sound and a ground reflection. When dealing with flyover scenarios close to residential areas, the interaction of sound with urban structures, especially reflection and diffraction, should be considered. Typical models for auralization in urban areas in fact do consider those interactions but neglect the inhomogeneity of the atmosphere. Thus, in this paper, the two models are combined in an approach to link between atmospheric models using curved propagation paths and urban models using straight paths but handling structure interaction.

Keywords: Outdoor sound propagation, Aircraft noise, Urban environment, Auralization, Open-source

1 Introduction

Noise in urban environments is an important issue to public health [1]. Proper noise regulation requires sophisticated models for sound propagation which are used for noise predictions. For example the Harmonoise model [2] was developed to produce noise maps in the European Union. One application is the prediction of aircraft noise, which is one of the major sound sources in residential areas close to airports [1]. The model focuses on the determination of sound pressure levels at observation points. However, it is known that noise evaluation based on energetic mean values is not sufficient to create an auditory impression of specific sound events. For example, Brambilla and Maffei [3] showed in their soundscape study that a reduced average sound pressure level does not necessarily lead to a more pleasant urban environment. Another reason is that in aircraft noise certification, the receiver is defined to be a microphone located at 1.2 m height above a free ground [4]. This is an appropriate procedure to measure aircraft noise in a rather reproducible way, but it is far from being realistic when it comes to the auditory impression for a human listener in the built environment.

In contrast, auralization is a tool which expands the scope of noise prediction enormously. Sound rendering for 3D auditory displays opens a new dimension of noise control and assessment. Accordingly, auralization models for urban noise and aircraft noise are in rapid development. By using appropriate models for source, sound propagation and receiver, a time-domain signal is calculated, which can be presented e.g. via headphones [5]. This approach allows

to listen to realistic scenarios including noise sources in a virtual environment. This again, enables a direct assessment of the perceived noise, e.g. in listening tests. Especially for dynamic scenes like aircraft flyovers, the underlying simulation for the sound propagation consumes a lot of resources. Thus, it is desired to use efficient methods which typically base on the principle of geometrical acoustics.

Several frameworks for the auralization of aircraft noise based on this principle exist. A typical approach is assuming straight sound paths [6–8], since this significantly reduces the computational effort. However, this neglects the inhomogeneity and movement of the atmosphere which influences the sound paths considerably as they lead to refraction and advection [9]. Generally, those effects are known to have an audible impact on the perceived sound [10]. Consequently, efficient methods for finding curved sound paths in a stratified, moving atmosphere [11, 12] have been introduced. A recently published study even suggests that a real-time auralization based on curved sound paths is possible [12]. All approaches mentioned above share the assumption of a horizontal plane for the ground reflection. Regarding aircraft noise in residential areas, this is a drawback since any interaction with the buildings – especially reflection and diffraction – is not considered.

Approaches to auralization of noise of urban areas include such an interaction to varying degrees. However, to the authors knowledge, all available methods assume straight sound paths which only is applicable if the considered sound sources are located within or close to the urban area. Some studies consider the shielding effect of barriers in addition to the ground reflection, e.g. for car pass-by noise

*Corresponding author: psc@akustik.rwth-aachen.de

[13] or wind turbine noise [14]. Aalmoes et al. [15] presented a model for the auralization of unmanned aerial vehicles (UAVs) flying through a city. Using a full 3D geometric model of the buildings, it considers reflections up to first order while neglecting edge diffraction. A more general approach was introduced by Tsingos et al. [16]. Their framework is capable of simulating sound paths with higher order reflections. Additionally, it considers diffraction up to first order including an approximation for the shadow region. Based on this approach, the so-called *image edge model* (IEM) [17] was recently introduced. By not only mirroring sources at walls but also mirroring edges, it is possible to simulate sound paths including higher order reflections, diffraction and respective combinations.

Aiming at auralization of aircraft noise in urban areas, it seems that solving the problems of atmospheric and urban sound propagation requires very different assumptions. To the authors' knowledge, there is no geometrical acoustic model which could consider both, refraction and advection caused by an inhomogeneous, moving medium as well as reflections and diffraction caused by urban structures. As the principles of the respective approaches differ significantly, considering both effects in a single algorithm seems impracticable. Hence, the present work introduces the so-called *virtual source method* (VSM). It serves as interface between curved sound paths in inhomogeneous, moving media and straight path models considering reflection and diffraction. An open-source version of this approach is provided combining the Atmospheric Ray Tracing framework [12] with the image edge model [17]. The sound paths resulting from such a combined simulation can be used as basis for the auralization of flyovers close to residential areas.

2 Virtual source method

The presented *virtual source method* is designed for the purpose of aircraft noise auralization but it might also be applied to other scenarios where the sound source is at a reasonable distance from the urban environment. Instead of relying on a single model considering both effects, it works as interface between the two simulation worlds. An open-source MATLAB implementation allows interfacing between the Atmospheric Ray Tracing (ART) framework [12] and the image edge model (IEM) [17] for linking sound propagation in the atmosphere with urban sound propagation. This implementation is part of the ITA-Toolbox [18]. A ready-to-use framework is provided in the [Supplementary material](#). This includes binaries of the respective simulation interfaces, ARTMatlab and [pigeon](#).

Considering a flyover scenario as shown in [Figure 1](#), aircraft are typically very far away from the urban environment if compared to the dimensions of the buildings. Additionally, they fly at a high altitude. Thus, it is a reasonable assumption that propagation effects caused by the inhomogeneity of the atmosphere, e.g. refraction, mainly influence the sound propagation path component which is

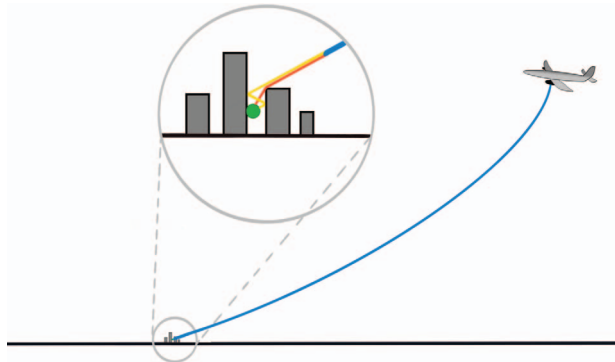


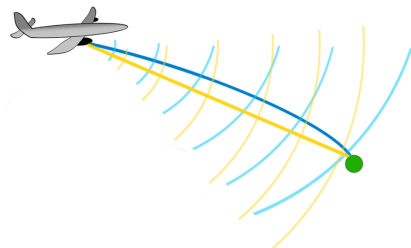
Figure 1. Sound paths during an aircraft flyover of an urban area. While propagating through the atmosphere, the sound paths are rather similar (blue). Within the urban area, the propagation paths significantly differ (yellow and red) due to interaction with the buildings.

outside of the urban domain. As the residual path length in the urban environment is by orders of magnitude shorter than the path length in the atmosphere, it can be assumed that those atmospheric effects do not change significantly between the different urban sound propagation paths. Accordingly, additional refraction effects in the urban sound paths can well be neglected. Broadly speaking, the sound paths connecting an aircraft with a receiver in an urban environment "share" the atmospheric propagation effects while the respective urban propagation effects (reflection, diffraction, scattering, attenuation) differ among them.

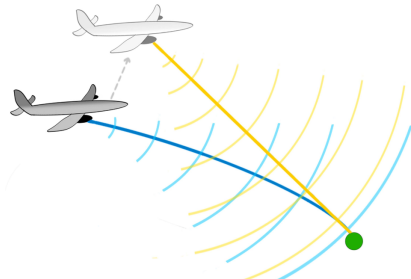
Thus, the virtual source method uses a single atmospheric sound path which is simulated under free field conditions using the ART framework. Based on the assumptions above, a virtual source position is defined which maintains the propagation delay and incident direction at the receiver for a homogeneous medium. This virtual source position is then used to carry out the simulation using the urban propagation model (IEM). The result is a set of straight sound paths including sequences of reflections and diffractions. Since those are simulated based on the virtual source, they already include the effects induced by the atmosphere. A detailed discussion on this procedure is given in [Section 2.1](#). For the actual auralization, we are not interested in the sound paths as such but in the acoustic parameters which can be derived from those paths (e.g. propagation delay, spreading loss and air attenuation). Since these parameters control the digital signal processing elements during the auralization process, they are called *auralization parameters* in the following. When using the virtual source method, those parameters require special processing which is discussed in [Section 2.2](#).

2.1 Virtual source position

As introduced above, the virtual source method provides an interface between the two simulation domains using a virtual source position for the urban model which



(a)



(b)

Figure 2. Comparison between homogeneous (yellow) and inhomogeneous (blue) free field paths with and without adjusting the source position; (a) Without adjustment of the source position; (b) With adjustment of the source position.

is derived from the result of the atmospheric propagation model. For the determination of this position, it is important to consider the respective assumptions regarding the atmosphere. While the Atmospheric Ray Tracing framework simulates curved sound propagation paths based on a stratified, moving atmosphere, the image edge model assumes a homogeneous, non-moving medium with straight sound propagation. This means that the ray direction of atmospheric sound propagation at the interface between the two models must be determined, so that the propagation can be smoothly continued into the urban environment domain. [Figure 2a](#) illustrates this phenomenon for a free field case.

For the auralization, significant features such as geometric spreading, air attenuation and propagation delay are directly based on those paths. The same holds for the launch direction at the source and incident direction at the receiver. The first is important when considering the source characteristics based on far-field directivities. The incident direction, on the other hand, is required for the three-dimensional sound reproduction at the receiver, e.g. using head-related transfer functions (HRTFs) or other spatial audio formats (such as Ambisonics). This is achieved by moving the source to a virtual position. As illustrated in [Figure 2b](#), this position is chosen so that the resulting direct path between source and receiver possesses the same incident direction and an equivalent length.

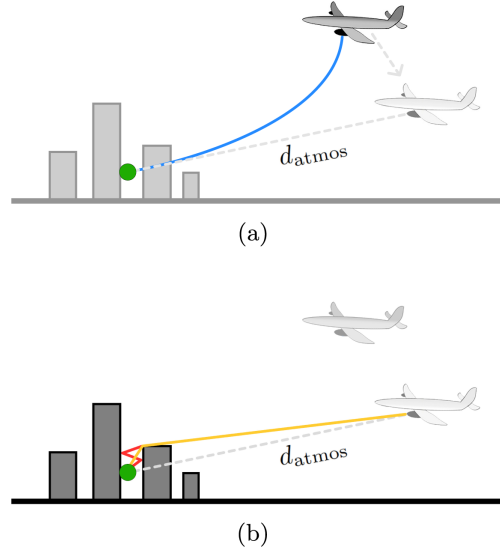


Figure 3. Procedure for the path simulation using the virtual source method. The virtual source is determined by converting the atmospheric free field path (blue) to an equivalent virtual path (dashed, grey). Then, the image edge model is used to determine the different urban paths (yellow and red) based on this virtual source. In this scenario, the direct path (dashed, grey) is blocked by a building and therefore inaudible. (a) Definition of virtual source based on an atmospheric free field path; (b) Determination of urban paths between virtual source and receiver.

[Figure 3](#) shows how the virtual source is determined in a given scenario. At first, the direct path is derived using the Atmospheric Ray Tracing framework by only considering atmospheric effects and neglecting the objects of the urban environment. Based on the propagation delay and incident direction of this path, the location of the virtual source is defined. For this purpose, a straight line starting at the receiver location is cast in the negative incident direction of the atmospheric path. The virtual source is located on that line at the distance d_{atmos} from the receiver which is determined using the corresponding propagation delay τ_{atmos} and the speed of sound c_{urban} used in the urban simulation domain:

$$d_{\text{atmos}} = c_{\text{urban}} \cdot \tau_{\text{atmos}}. \quad (1)$$

In our case, c_{urban} is chosen to match the parameter of the stratified atmosphere at receiver altitude.

Using the virtual source position for the urban simulation, the incident direction and the propagation delay of the inhomogeneous atmosphere is indirectly included for all paths. However, the geometric spreading, air attenuation and launch direction at the source require special treatment as will be discussed in [Section 2.2](#). In this context, it should be noted that the distance between virtual source and receiver could also be computed based on the geometric spreading loss. While in a homogeneous medium, propagation delay and spreading loss are directly related by the distance, this does not hold for the inhomogeneous case. Thus, the virtual source position can only be optimized for

one of those parameters. In the course of this work, both approaches were tested and lead to similar results. We decided to use the propagation delay, as it is used to generate Doppler shifts during the auralization process and small fluctuations in this parameter can easily lead to audible artifacts.

2.2 Auralization parameters

When deriving the auralization parameters from the resulting urban paths, only propagation delay and incident direction properly consider the atmospheric propagation, as those were used to calculate the virtual source position. Spreading loss, air attenuation and launch direction at source require adjustment based on the respective atmospheric free field parameter. Parameters related to structure interaction, namely reflection and diffraction filters, do not require this procedure, since they are only part of the urban simulation. Thus, they are not discussed here. An overview on the general approach is given in Figure 4. In the following, the procedures for determining the individual auralization parameters are discussed in detail.

Propagation delay

The propagation delay of an urban path τ_{path} can be computed similar to equation (1). In this case, the overall path length l_{path} is relevant, which can be determined accumulating the length of the respective path segments (see Fig. 5):

$$\tau_{\text{path}} = \frac{l_{\text{path}}}{c_{\text{urban}}} . \quad (2)$$

Geometric spreading

A typical approach when assuming a homogeneous medium and dealing with point source as done in the image edge model, is using the distance law ($1/d$ -law) to determine the spreading loss. For the atmospheric simulation using an inhomogeneous medium, however, the spreading loss $g_{\text{spread, atmos}}$ is calculated based on the Blokhintzev invariant [19] (also see Eqs. (12) and (13) in [12]). Since $g_{\text{spread, atmos}}$ is not considered when determining the distance between virtual source and receiver d_{atmos} , there is a mismatch between those parameters, i.e. $g_{\text{spread, atmos}} \neq 1/d_{\text{atmos}}$. Thus, the distance law is normalized for the urban paths using

$$g'_{\text{spread, path}} = \frac{g_{\text{spread, atmos}}}{1/d_{\text{atmos}}} \cdot \frac{1}{l_{\text{path}}} . \quad (3)$$

Using this formula, the spreading loss factors for the direct urban and atmospheric path match again. For all other urban paths, the spreading loss increases (the factor decreases) in accordance with the distance law.

If an urban path contains a diffraction, the distance law cannot be applied anymore. Instead, the spreading loss is based on the following formula which is part of the UTD (see Eq. (23) in [20]):

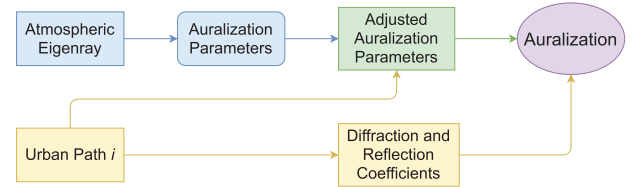


Figure 4. Block diagram for determining auralization parameters based on the paths found by the virtual source method.

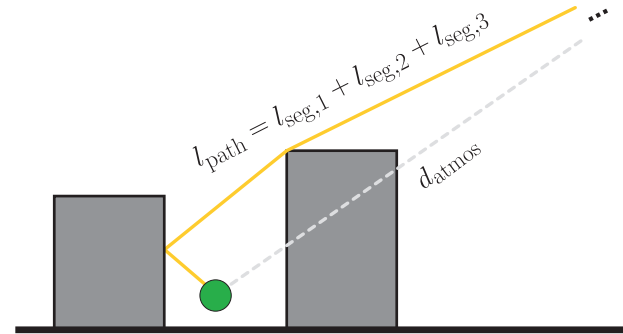


Figure 5. When calculating the auralization parameters based on an urban path, the overall path length l_{path} and the distance between virtual source and receiver d_{atmos} are relevant.

$$g_{\text{spread, path}} = \sqrt{\frac{s'}{s(s' + s)}} . \quad (4)$$

Here, s' denotes the distance between the source and the first point of diffraction (first apex point), whereas s describes the distance between this point and the receiver. Using the same normalization approach as before, the spreading loss factor for paths including diffraction becomes

$$g'_{\text{spread, path}} = \frac{g_{\text{spread, atmos}}}{1/d_{\text{atmos}}} \cdot \sqrt{\frac{s'}{s(s' + s)}} . \quad (5)$$

Air attenuation

In the Atmospheric Ray Tracing (ART) framework, the medium attenuation is determined by integrating the frequency-dependent absorption coefficient $\alpha_{\text{air}}(f)$ [dB/m] defined in ISO 9613-1 [21] along a curved sound path. Again, the attenuation for the urban paths of the combined model is obtained by adjusting the respective parameter of atmospheric free field path $A_{\text{air, atmos}}(f)$ [dB]. Assuming the properties of atmospheric propagation are the same for all urban paths, there is an additional attenuation depending on the path length difference compared to the direct path

$$\Delta l = l_{\text{path}} - d_{\text{atmos}} . \quad (6)$$

While further propagating through the urban area, the air attenuation is assumed to be constant along the sound path (homogeneous medium). Similar to the speed of sound, the atmospheric properties are evaluated at receiver altitude for

this purpose. Then, the air attenuation for an urban path becomes:

$$A_{\text{air, path}}(f) = \alpha_{\text{air}}(f) \cdot \Delta l + A_{\text{air, atmos}}(f). \quad (7)$$

Launch direction at source

In the context of auralizing aircraft noise, it is also important to consider the source directivity [22]. During the auralization process, the proper directivity function can be applied using the launch direction (elevation Θ_{launch} and azimuth ϕ_{launch}) at the source. Compared to the curved sound path of the atmospheric model, the launch direction of the free field path using the virtual source mismatches. This can be corrected rotating the virtual source as shown in Figure 6. For this purpose, the angle offsets between the atmospheric path ($\Theta_{\text{launch, atmos}}, \phi_{\text{launch, atmos}}$) and the direct path based on the virtual source ($\Theta_{\text{launch, direct}}, \phi_{\text{launch, direct}}$) are determined:

$$\Delta\Theta_{\text{launch}} = \Theta_{\text{launch, atmos}} - \Theta_{\text{launch, direct}}, \quad (8)$$

$$\Delta\phi_{\text{launch}} = \phi_{\text{launch, atmos}} - \phi_{\text{launch, direct}}. \quad (9)$$

3 Proof of concept

As discussed in Section 2, it is assumed that the atmospheric propagation effects do not change significantly among the different urban paths. Thus, the virtual source position is based on a single atmospheric path directly connecting source and receiver (free field path). This simplification could introduce inaccuracies regarding multiple properties of the higher order paths based on the virtual source. As demonstrated in Figure 7, the incident angles at the respective points of first interaction may not match those of the corresponding atmospheric paths. Moreover, a mismatch might also occur for the auralization parameters described in Section 2.2.

The aim of this section is to estimate the error that is introduced by this assumption. To the authors' knowledge, a benchmark for a complex aircraft flyover scene including atmospheric and urban propagation effects does not exist. Thus, the workaround is that the atmospheric effects for higher order urban paths are compared to results obtained with additional rays simulated using the ART framework. These atmospheric paths are computed using the real source position and the first interaction point (point of reflection or diffraction) of each urban path as receiver. The resulting rays are compared to the respective urban paths regarding their auralization parameters. To ensure a proper comparison, the urban paths are truncated after the first interaction point. This comparison is carried out for multiple source positions of a simple flyover scenario described in Section 3.1. Then, the results are presented in Section 3.2.

It should be noted that the given procedure does not replace a comparison with a proper benchmark, since it neglects the influence of the urban structure on the

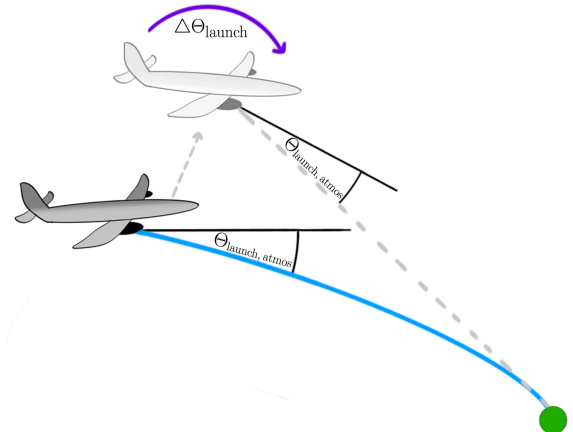


Figure 6. The virtual source is rotated to maintain the launch angles of the atmospheric path.

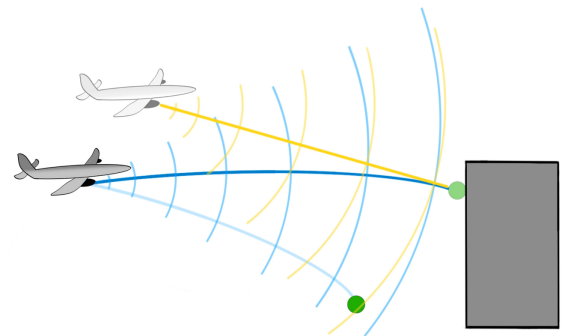


Figure 7. Comparison of incident directions between an urban path and a new atmospheric path to the first interaction point of the former.

atmospheric properties. In a real scenario, urban structures would have an impact on the weather conditions, e.g. wind. Thus, the assumption of a stratified atmosphere would not hold anymore, at least in the vicinity of the ground. In other words, the buildings still have an indirect impact on sound propagation even though a direct interaction did not (yet) happen. Although the present investigation does not account for this phenomenon, it currently is the most suitable option to access the accuracy of the virtual source method. In contrast to using a numerical simulation as benchmark, one advantage of this approach is the capability of comparing individual auralization parameters, especially the propagation direction, instead of a combined acoustic result like a transfer function.

3.1 Flyover scenario

To assess the accuracy of the virtual source method, its simulation results are examined for a typical flyover scene. The scenario is based on an aircraft take-off trajectory generated with the *MICADO* software [23]. It is the same trajectory previously used to evaluate the performance of the Atmospheric Ray Tracing framework (see Sect. 3.2 in [12]). The central portion of the trajectory as illustrated

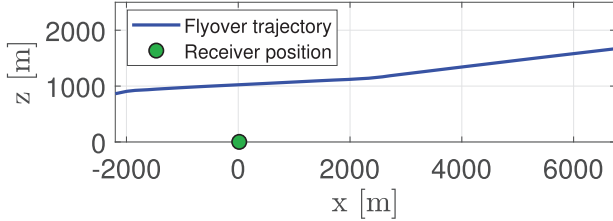


Figure 8. Aircraft flight trajectory generated with the MICADO software [23].

in [Figure 8](#) is used here. Meanwhile, the stationary receiver resides at a distance of 6.5 km from the starting point of the original trajectory, at the position [0, 0, 1.8] m. This is in concordance with the ICAO standard for flyover measurements [4]. However, the receiver height is slightly increased to match the head position of a standing human listener. Also the parameters of the stratified, moving atmosphere are taken from the flyover scenario in [12]. This includes the International Standard Atmosphere (ISA) temperature profile [24] and a logarithmic wind profile [25]. The wind orientation is set to the negative x -direction so that the aircraft moves upwind, which is a common procedure for take-offs [26]. In order to reduce the uncertainty caused by the algorithm for finding eigenrays, the receiver radius is chosen to 2.5 cm instead of using the default of 1 m.

For the urban simulation using the virtual source and image edge model, a simple street canyon is placed around the receiver. The model is created using the *SketchUp* software. As shown in [Figure 9](#), the receiver is located centrally between the two identical buildings with dimensions $10 \times 10 \times 255$ m. As for the simulation settings, the maximum combined path order is set to 3 and the maximum order for reflection and diffraction is 2 respectively. Thus, an urban path of maximum order either has two reflections and one diffraction or vice versa. To reduce computation times, back-face culling and occlusion detection [17] are used. A full list of the simulation settings used for the respective frameworks is provided in the [Supplementary material](#).

[Figure 10](#) shows the resulting virtual source and sound paths for a single position on the aircraft trajectory. An animation of the full flyover is provided in a [video](#). It also includes an auralization of the scenario as described in [Section 5](#).

3.2 Uncertainty of auralization parameters

As introduced above, the simulation accuracy of the virtual source method is assessed by comparing its urban paths to newly computed atmospheric paths. The corresponding procedure is as follows: First, the virtual source and resulting urban paths are determined for each source location of the flyover scenario described in [Section 3.1](#). Then, the first interaction point of each path is detected and new atmospheric paths to these points are simulated. To quantify the uncertainty introduced by the virtual source method, the urban path segments up to those interaction points are compared to the corresponding atmospheric paths

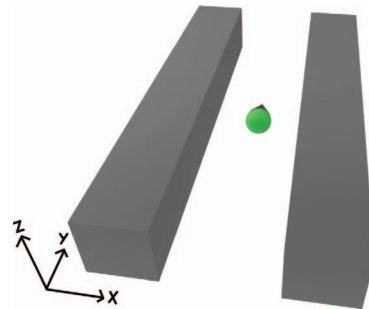


Figure 9. Visualization of the city model used for the flyover scenario.

regarding their auralization parameters. For this purpose, the deviation of those parameters is evaluated for each position on the trajectory and each of the 69–120 urban paths.¹ In addition to the parameters introduced in [Section 2.2](#), also the incident azimuth and elevation at the intersection points are considered.

In the course of this investigation, the parameters showing the most significant deviation are the elevation angle of sound incidence, the spreading loss and the propagation delay. The respective errors are calculated using the following equations:

$$\Delta\Theta_{\text{in}} = \Theta_{\text{in}, \text{VSM}} - \Theta_{\text{in}, \text{ART}}, \quad (10)$$

$$\Delta A_{\text{spread}} = A_{\text{spread}, \text{VSM}} - A_{\text{spread}, \text{ART}}, \quad (11)$$

$$\Delta\tau = \tau_{\text{VSM}} - \tau_{\text{ART}}. \quad (12)$$

Here, Θ_{in} , A_{spread} and τ refer to the elevation angle of sound incidence at the receiver, spreading loss in dB and the propagation delay, respectively. The index ART refers to the new atmospheric paths simulated using the Atmospheric Ray Tracing framework. On the other hand, the index VSM refers to the urban path segments based on the virtual source method.

Based on equations (10)–(12), the parameter deviation is statistically evaluated among the urban paths for each source position on the trajectory. For this purpose, the median, the quantiles as well as the minimum and maximum deviation are determined. The results are shown in [Figure 11](#) along with the number of valid sound paths. Generally, the error increases with distance between aircraft and receiver. This makes sense, as the influence of the refraction on the sound path increases with propagation distance. The highest deviation occurs when the launch elevation angle at the source is closest to horizontal. This is the case in the beginning of the trajectory, where the aircraft resides at a lower altitude and the distance to the receiver is large. As a result, the refraction caused by the wind gradient is particularly strong [9, 11, 12].

Considering the elevation angle ([Fig. 11a](#)), the maximum deviation is 2.5° at the beginning of the trajectory.

¹Note that the number of valid sound paths depends on source and receiver position.

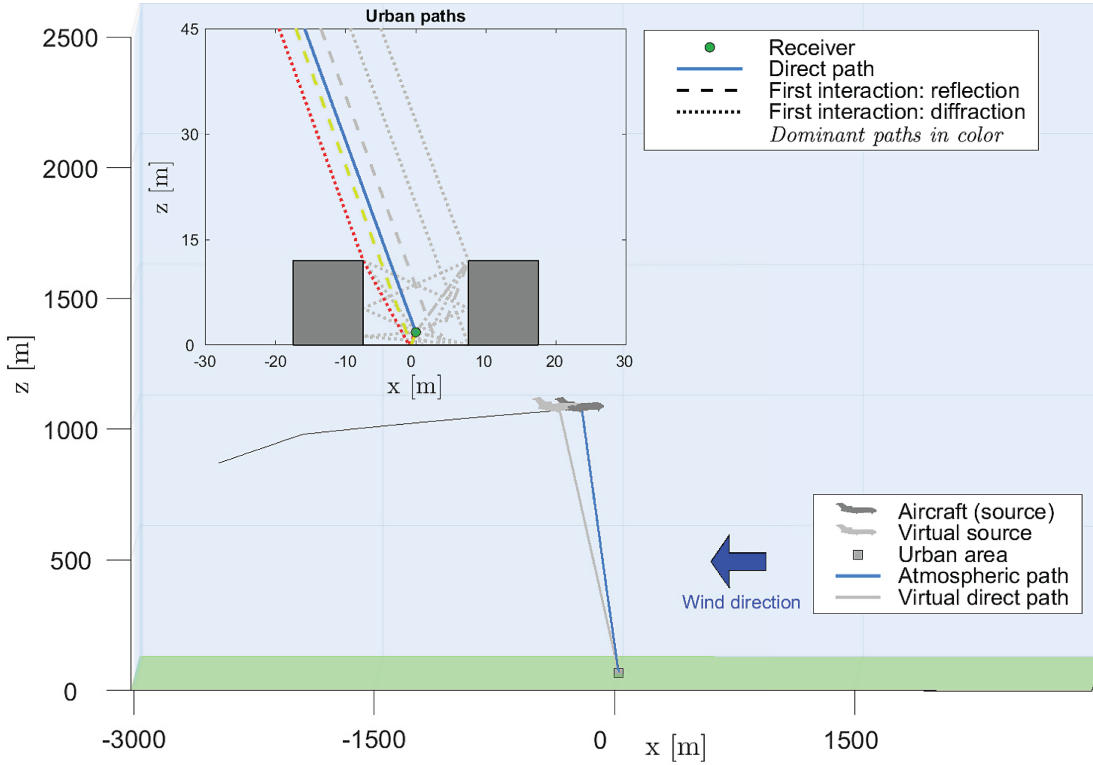


Figure 10. Virtual source and atmospheric and urban paths at 29 s flight time on the trajectory.

The influence of this error can be estimated in a worst-case scenario, where only a single path is considered. In this scenario, the respective path has just a single reflection. Then, the error of the incident angle at the point of reflection leads to a similar error at the receiver. According to Blauert [27], the localization blur in the median plane is at least 9°. Thus, the deviation of the incident angle at a reflection point should not affect the localization for the considered flyover. However, it might still lead to a change of coloration as different filters are used for the spatial reproduction, e.g. head-related transfer functions (HRTF) for binaural reproduction. This again, requires the utilized spatial reproduction system to support an accordingly high resolution. Secondly, the deviation of the incident elevation could have an effect on diffracted paths. Using the uniform theory of diffraction, the corresponding filter depends on the incident angle and has a stronger shadowing effect at high frequencies [16]. Thus, this filter might deviate particularly for horizontal edges and higher frequencies. For both cases, however, it is questionable whether such a small change in incident direction leads to audible changes in the overall result, especially considering that the number of contributing sound paths is relatively high and these urban sound paths are subject to additional spectral changes, e.g. caused by air attenuation and reflection.

Looking at Figure 11b, the spreading loss error is close to zero dB for most aircraft positions. Only at the beginning of the trajectory, it comes close to the *just noticeable difference* (JND) for sound pressure levels of 1dB [28]. Considering a single path, the virtual source method might introduce

audible differences with respect to the spreading loss for these aircraft positions. However, as discussed before, the overall auralization result is based on a composition of many sound paths considering additional acoustic effects. It is not yet clear whether this deviation is audible in this context.

The deviation of the propagation delay is shown in Figure 11c. The maximum deviation for the considered scenario is 1.2 ms. Setting this in relation to the overall delay of the sound paths, this corresponds to approximately 0.01%. Thus, it is unlikely that this effect will be perceived in terms of a “temporal shift” of the incoming sound. However, as soon as multiple paths are combined, their interference pattern might be affected. This phenomenon is further investigated in the following.

The errors in the propagation delay of individual sound paths have an influence on the interference pattern of a combined result. A typical example is the comb filter effect, which is caused by two interfering sound paths having a different propagation delay. A change of this delay difference leads to a shift of the spectral pattern of peaks and notches. If the interference pattern is created by a large number of sound paths, it becomes more complex. To investigate such an influence, the transfer functions (TFs) are calculated based on the virtual source method for each source position of the scenario described in Section 3.1. A second set of TFs is calculated using adjusted propagation delays for each sound path based on the results of Figure 11c. Figure 12 shows an exemplary pair of TFs for the first aircraft position, which refers to rather high deviation of the propagation

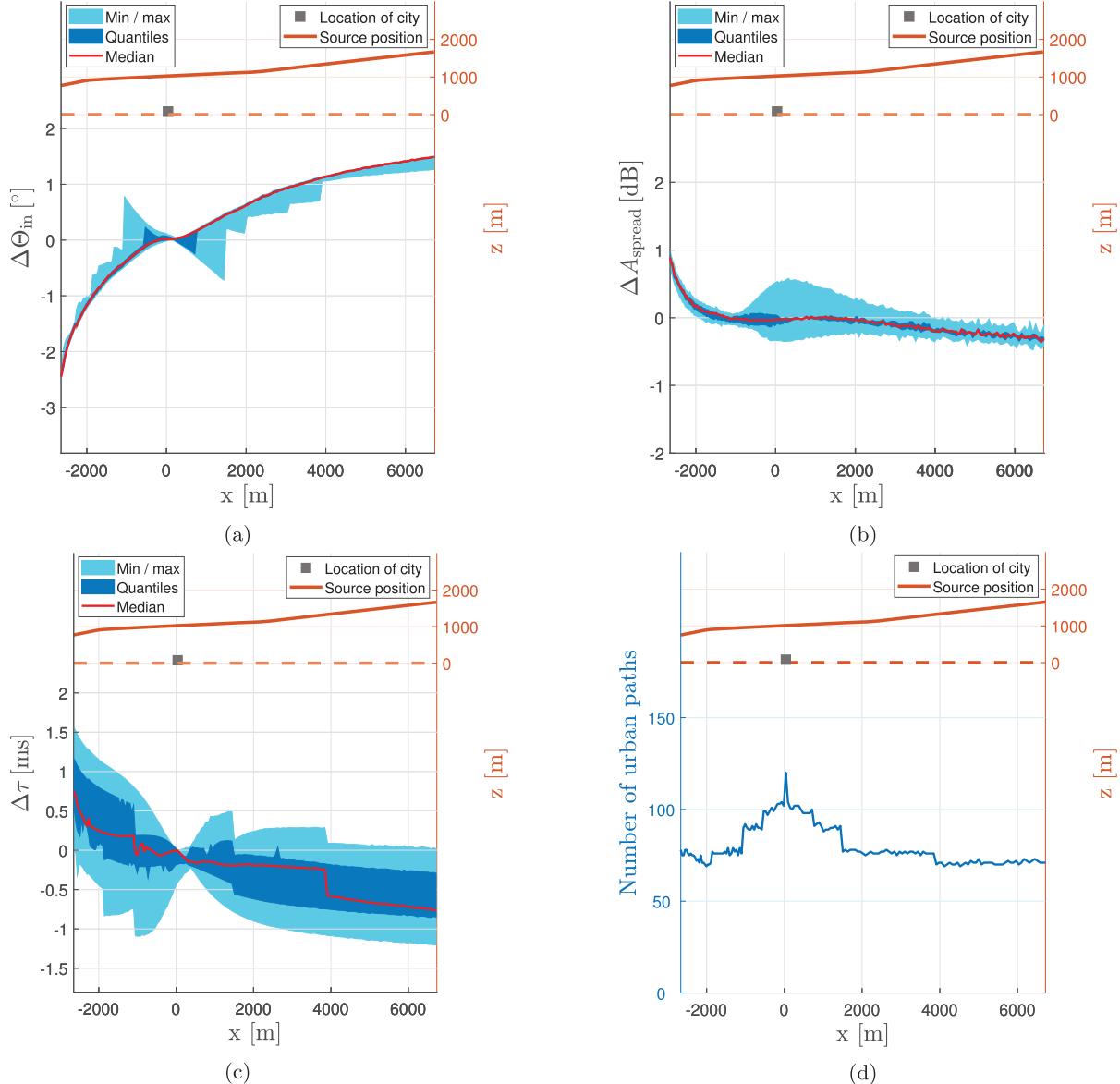


Figure 11. Difference in incident elevation angle and spreading loss between the atmospheric and urban paths to the first interaction points. (a) Elevation angle at the first interaction points; (b) Spreading loss; (c) Propagation delay; (d) Number of paths.

delays. It can be seen, that the respective patterns are very similar at low frequencies. More prominent differences can be observed above 600 Hz. Nevertheless, the general trend of the TFs is not changed when adjusting the propagation delays. To further quantify those differences, the two sets of TFs are convolved with an aircraft source signal based on the model by Dreier and Vorländer [29]. Using a 2-second steady-state excerpt of each output signal, the psychoacoustic parameters loudness, specific loudness and sharpness are evaluated using the Matlab routines based on DIN 45631:1991 [30] and DIN 45692:2009 [31], respectively. The two parameters follow a similar trend for both TF sets as shown in Figure 13. The mean deviation between the two approaches is 0.35 sone and 0.001 acum (respective standard deviations 1.14 sone/0.0114 acum) for absolute values of

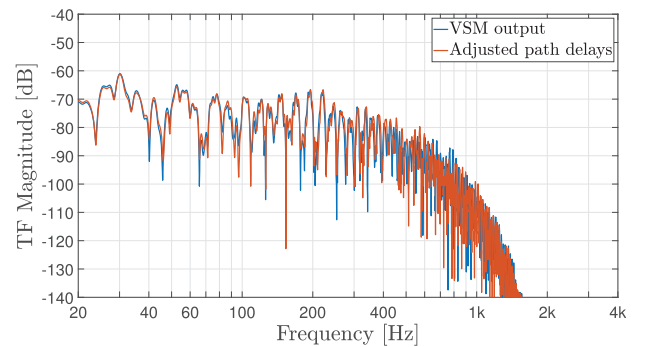


Figure 12. Exemplary transfer functions (TF) pair based on a combined simulation using the virtual source method. The second TF is calculated using an adjusted propagation delay for each path using the results from Figure 11c.

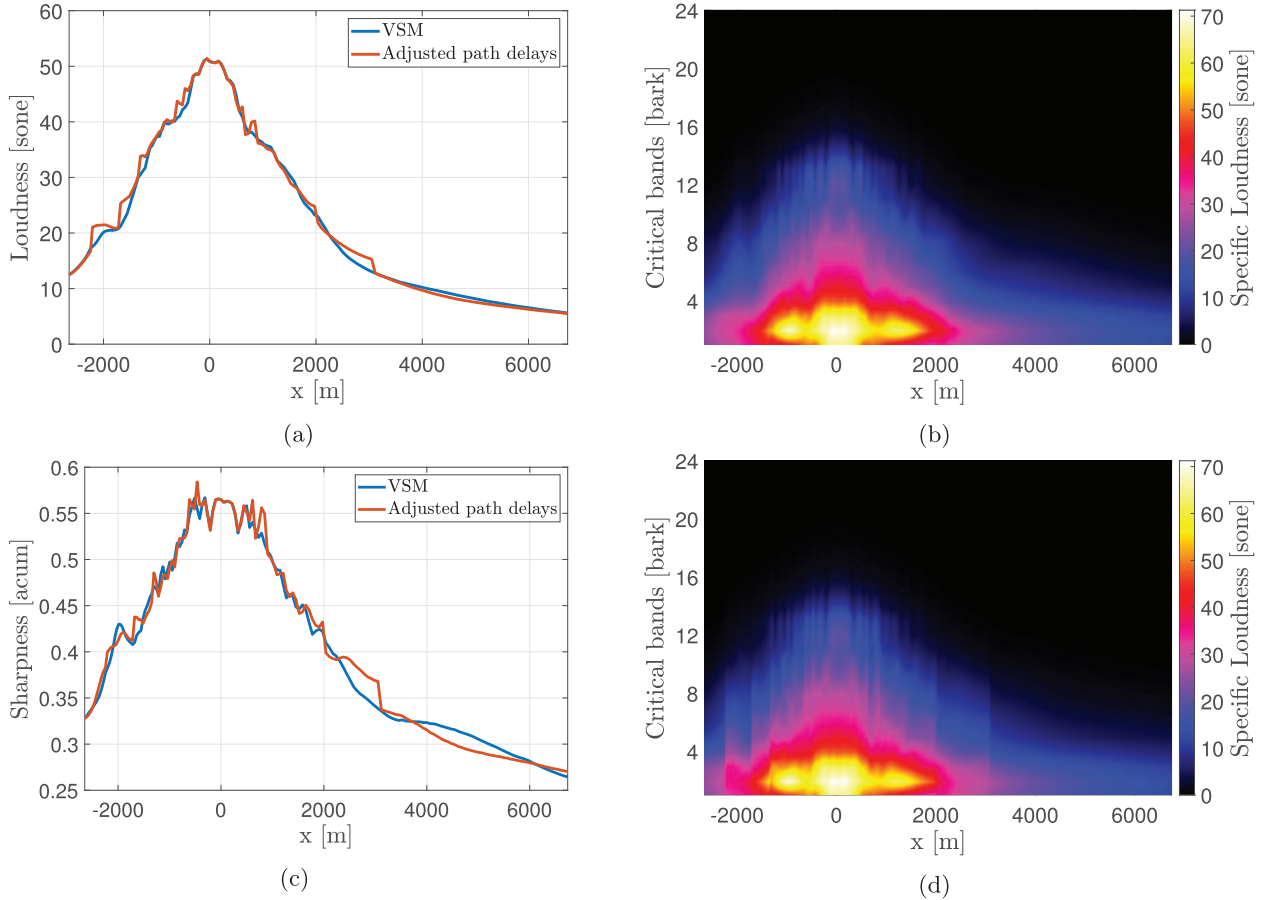


Figure 13. Comparison of two sets of transfer functions (TFs) based along the aircraft trajectory (x -component) regarding the psychoacoustic parameters loudness and sharpness. The first set of TFs is based on the sound paths from the virtual source method (VSM). The TFs of the second set are based on an adjusted propagation delay for each sound path according to Figure 11c. (a) Loudness; (b) Specific loudness (VSM); (c) Sharpness; (d) Specific loudness (adjusted path delays).

loudness and sharpness of 10–50 sone and 0.35–0.55 acum, respectively.

Generally, it should be considered that the interference pattern is influenced by additional effects. For example, reflections include frequency-dependent energy losses. In the example discussed here, all boundaries were assumed to be rigid, which leads to a worst-case interference pattern. Another example is turbulence, which leads to time-variant phase fluctuations. Those fluctuations differ between the sound paths (coherence loss) and therefore lead to less pronounced interference dips [32]. A recent study showed that the coherence loss can even dissolve the pattern caused by the interference of direct sound and ground reflection for larger aircraft-receiver distances at frequencies below 2 kHz [33]. It is therefore assumed that the effect of potential propagation delay errors on the overall spectrum does not reduce the plausibility of the auralization result.

Summarizing the uncertainty discussion, it is possible that the simplifications used for the virtual source method might introduce audible changes in the auralization parameters of individual sound paths. The most significant errors occur if the aircraft is farther away from the receiver when the launch direction is close to horizontal and the refraction

of the atmospheric ray is particularly strong. Considering a flyover scenario, however, those positions are of less interest than the positions closer to the receiver. Nevertheless, the absolute errors are still quite low. Since in a real scenario the contribution of each sound path is superposed with time-variant phase and amplitude changes caused by turbulence, it can be expected that the individual deviation of the auralization parameters do not reduce the plausibility of a resulting audio signal.

Other auralization parameters do have uncertainties, too. Those are negligibly small for the considered scenario. For instance, the error of the incident azimuth angle is below 10^{-4} degrees for the entire trajectory. Similarly, the deviation of the launch azimuth and elevation angle are smaller than 0.1° . For both, HRTFs and directivities, an equiangular resolution of 1° already is considered as high resolution. Higher resolutions are typically not used in practice. Thus, it is a reasonable assumption that the deviation of those parameters does not significantly affect the auralization result. Also for the air attenuation, the differences are negligible. For example, the maximum absolute deviation is approx. 0.5 dB at 4 kHz. For higher frequencies, the absolute value of air attenuation outweighs the actual

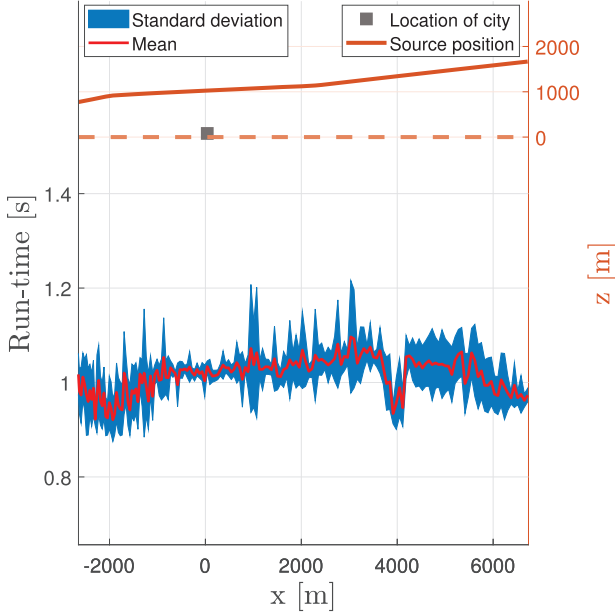


Figure 14. Simulation run-time per source position of the scenario described in Section 3.1. Each run-time refers to a combined simulation using Atmospheric Ray Tracing, the virtual source method and the image edge model.

uncertainty of this parameter (e.g. 1.5 dB deviation at 8 kHz compared to approx. 75 dB air attenuation).

4 Computational effort

To give a rough idea of the computational effort of the simulation approach, the run-time is measured for the aircraft flyover scenario from Section 3.1 using a typical work station computer. As shown in Figure 14, the run-time for simulating a single source/receiver position is between 0.8 s and 1.2 s. Currently, the virtual source method is implemented in Matlab while the individual simulation frameworks are implemented in C++. Thus, a lot of computation time is spent transferring data, e.g. the simulation results, between those two domains. The overall performance would be significantly higher, if all simulation steps were implemented in C++. When auralizing dynamic scenarios with the current framework, one simulation is carried out for each audio block. The simulations are carried out in advance for the whole aircraft trajectory before starting the actual auralization process. Nevertheless, this precalculation can be carried out in a reasonable time. For example, simulating the data for the scenario described in Section 5 (audio length of 83 s with 3900 blocks) takes roughly 1 h.

5 Aircraft flyover auralization

Using the *Virtual Acoustics* (VA) auralization framework [34], the flyover scenario described in Section 3.1 is auralized based on the sound paths generated with the

virtual source method. For this purpose, the respective auralization parameters introduced in Section 2.2 are determined for every point of the trajectory and stored. During the actual auralization process, the auralization parameters are sent to VA controlling the respective digital processing elements. This approach allows to auralize scenarios where the listener resides at a fixed position but can freely move the head. To increase the performance of the signal processing, air attenuation and diffraction filters are processed using one-third octave band magnitude spectra. Thus, the phase of the diffraction filter is omitted here. However, in dynamic scenarios, temporal phase changes of 180° play an important role when reflected and diffracted sound paths complement each other. Those phase changes are indirectly considered by changing the sign of the signal gain corresponding to the respective diffracted sound path.

The presented scenario, is rendered using a sampling rate of 44100 Hz and a block size of 1024 samples. Assuming a similar simulation run-time as shown in Figure 14, this corresponds to a real-time factor of approx. 50. However, to allow for an interpretation of the effects observed, the maximum combined path order of the urban simulation is reduced to two while maximum reflection and diffraction orders are both set to one in this case. A spatial impression of the scene is given using binaural reproduction. As previously shown in Figure 9, the listener orientation is set to the positive *y*-direction. Hence, the aircraft is initially located to the left of the listener and later passes the receiver before travelling further to its right. The resulting auralization is available in a [video](#), which also shows the virtual source position and the sound paths in the urban area.

The video underlines that considering reflections and diffraction for auralization of aircraft flyovers close to urban areas is of great importance. Although the aircraft is flying from left to right, in the audio it seems to be located on the right side at first. This is because the direct path is blocked by the left building and the most dominant sound path is the reflection on the right building. At around 25 s, the perceived aircraft location seems to transition to the left side as the direct sound path becomes audible. This effect starts being reversed at approximately 42 s when the direct path becomes inaudible and the reflection at the left building kicks in. These effects can obviously only be reproduced when the urban structures are considered for the sound path simulation. Furthermore, the video showcases the influence of the inhomogeneity on the sound paths. Especially at the beginning and the end of the aircraft trajectory, the refraction of the atmospheric path is particularly strong so that the distance between virtual source and aircraft is up to 360 m and 460 m, respectively.

However, the current approach has limitations regarding the transitions between urban sound paths. Whenever a rather dominant sound path becomes audible or inaudible, the rendered audio has small artifacts. This is likely caused by only considering the phase of the diffraction filters indirectly. Future work should investigate the auralization process based on the introduced virtual source method in more detail.

6 Summary and conclusion

In this paper, the virtual source method (VSM) is introduced. It allows to interface between geometric acoustic simulations of atmospheric and urban sound propagation. Individually, the respective approaches use very different assumptions: For the atmospheric simulations, the focus lies on the curved sound propagation due to the inhomogeneity of the medium only considering direct sound and ground reflection. For the urban simulation, a homogeneous medium is assumed but reflections and diffraction of higher order can be considered. The presented method derives a virtual source position based on the result of the atmospheric simulation under free-field conditions, which serves as interface to the urban simulation. In this way, the resulting straight sound paths indirectly contain properties of the atmospheric simulation. An open source implementation is available for Matlab combining the Atmospheric Ray Tracing framework [12] and *pigeon* which is based on the image edge model [17].

The combined simulation was tested using an aircraft flyover scenario after a take-off and a simple urban environment with two buildings. Since a benchmark scenario is not available yet, the resulting straight sound paths were compared to additional curved paths traced to the respective first points of interaction regarding acoustic parameters derived from the sound paths. For launch direction at the source and air attenuation, the respective errors are negligible. This is not the case for spreading loss, propagation delay and incident direction at the receiver. Although the respective errors are relatively small, they cannot be neglected generally, e.g. by comparing with a just noticeable difference. However, given their low magnitude, they are not expected to reduce the plausibility of the results, at least if considering each path individually. In this context, it should be noted that the respective errors mainly appear at the edges of the trajectory. These distant positions are generally less relevant for flyover noise assessments, since the noise level is much lower compared to the situation when the aircraft is closest to the receiver.

When superposing multiple sound paths, however, a variation of the respective propagation delays can affect the frequency-domain interference pattern. Thus, the influence of the estimated propagation delay error on this pattern was investigated. For this purpose, transfer functions (TFs) were calculated based on the auralization parameters taken from the virtual source method for each considered aircraft position. A second set of TFs was calculated modifying the propagation delay for each sound path based on the estimated errors. The two TF sets were convolved with an aircraft signal and compared evaluating the psychoacoustic parameters loudness and sharpness. The results follow a very similar trend and the mean deviation of the psychoacoustic parameters is rather low. Moreover, in a real scenario, the interference pattern would be less prominent due to non-rigid boundary conditions and the coherence loss caused by turbulence. This effect typically causes dynamic phase jitter in the same order of magnitude as the stochastic delay uncertainty of the propagation path

filters. It therefore is a reasonable assumption that the individual path deviation of the auralization parameters do not reduce the plausibility of the resulting audio signal as such, although authenticity cannot be achieved.

Using the same scenario as for the investigations above, the aircraft flyover was auralized. The resulting audio underlines how considering reflections and diffraction at urban structures, increases the realism significantly. This holds particularly regarding the localization of the source when the direct path is occluded, so that secondary sound paths become dominant.

Next steps towards improvements and extensions are planned or in progress. A large scale project including an experimental benchmark for the urban model is going to start soon. This includes listening tests with variants of diffraction filters in order to optimize computational effort with reference to perception. Also, inclusion of surface scattering is relevant when it comes to complex building facades with roughness texture on various scales. Regarding atmospheric propagation, turbulence is an important aspect, which can be included in the auralization process using time-variant filters. While this was successfully done for auralizations based on the Atmospheric Ray Tracing framework alone where only two sound paths are considered, this is ongoing work for the presented approach. Finally, the combination of the aircraft sound component with that of other sound sources in urban environments will lead to the ultimate goal of establishing an open-source Virtual Reality toolbox for soundscape research.

Acknowledgments

The authors would like to express their gratitude to the German Research Foundation (DFG, Deutsche Forschungsgemeinschaft) for funding the project *Auralization of Urban Environments – Real-time Simulation of Diffraction* under grant number VO 600/39-1, which made this contribution possible. Additionally, the authors would like to thank Jonas Stienen for his insights and support regarding the image edge model.

Supplementary material

The supplementary material of this article is available at <https://acta-acustica.edpsciences.org/10.1051/aacus/2022021/olm>.

The supplementary material of this paper allows to run the simulations and reproduce the data-based plots presented here. Running the respective code requires a working Matlab version. Additional requirements are inherited by the ITA-Toolbox. A copy of the utilized ITA-Toolbox version including the implementation of the virtual source method is provided. Additionally, the data contains the frameworks used for the atmospheric and urban simulation, namely *ARTMatlab v2021b* and *pigeon v2021a*. Finally, a video of the presented aircraft flyover including the auralization from Section 5 is available [here](#). The video shows

the atmospheric sound path as well as the the virtual source position and the respective urban sound paths.

References

1. World Health Organization (WHO): Environmental noise guidelines for the European Region. 2018.
2. E. Salomons, D. Van Maercke, J. Defrance, F. de Roo: The harmonoise sound propagation model. *Acta Acustica* 97, 1 (2011) 62–74.
3. G. Brambilla, L. Maffei: Perspective of the soundscape approach as a tool for urban space design. *Noise Control Engineering Journal* 58, 5 (2010) 532.
4. ICAO: Environmental technical manual, Volume I – Procedures for the Noise Certification of Aircraft, Standard, International Civil Aviation Organization. 2018.
5. M. Vorländer: Auralization: Fundamentals of acoustics, modelling, simulation, algorithms and acoustic virtual reality. RWTH edition (2nd ed.), Springer International Publishing, Cham, 2020.
6. S.A. Rizzi, A.R. Aumann, L.V. Lopes, C.L. Burley: Auralization of hybrid wing-body aircraft flyover noise from system noise predictions. *Journal of Aircraft* 51, 6 (2014) 1914–1926.
7. A. Sahai, F. Wefers, S. Pick, E. Stumpf, M. Vorländer, T. Kuhlen: Interactive simulation of aircraft noise in aural and visual virtual environments. *Applied Acoustics* 101 (2016) 24–38.
8. R. Pieren, L. Bertsch, D. Lauper, B. Schäffer: Improving future low-noise aircraft technologies using experimental perception-based evaluation of synthetic flyovers. *Science of The Total Environment* 692 (2019) 68–81.
9. V.E. Ostashev, D.K. Wilson: Acoustics in moving inhomogeneous media, 2nd ed., CRC Press, Boca Raton, USA. 2016.
10. O. Reynolds: On the refraction of sound by the atmosphere. *Proceedings of the Royal Society of London* 22 (1874) 531–548.
11. M. Arntzen, S.A. Rizzi, H.G. Visser, D.G. Simons: Framework for simulating aircraft flyover noise through nonstandard atmospheres. *Journal of Aircraft* 51, 3 (2014) 956–966.
12. P. Schäfer, M. Vorländer: Atmospheric ray tracing: An efficient, open-source framework for finding eigenrays in a stratified, moving medium. *Acta Acustica* 5 (2021) 26.
13. P. Thomas, M. Boes, T. Van Renterghem, D. Botteldooren, M. Hornikx, W. Desmet, M. Nilsson: Auralisation of a car pass-by behind a low finite-length vegetated noise barrier, in: Proceedings of the 9th European Conference on Noise Control. 2012, pp. 932–937.
14. K. Heutschi, R. Pieren, M. Müller, M. Manyoky, U.W. Hayek, K. Eggenschwiler: Auralization of wind turbine noise: Propagation filtering and vegetation noise synthesis, *Acta Acustica united with Acustica* 100, 1 (2014) 13–24.
15. R. Aalmoes, M. van der Veen, H. Lania: Auralization of aircraft noise in an urban environment, in Proceedings of the 23rd International Congress on Acoustics, Aachen, Germany. 2019, pp. 1659–1666.
16. N. Tsingos, T. Funkhouser, A. Ngan, I. Carlstrom: Modeling acoustics in virtual environments using the uniform theory of diffraction, in Proceedings of the 28th Annual Conference on Computer Graphics and Interactive Techniques – SIGGRAPH '01, ACM Press, New York, USA. 2001, pp. 545–552.
17. A. Erraji, J. Stienen, M. Vorländer: The image edge model. *Acta Acustica* 5 (2021) 17.
18. M. Berzborn, R. Bomhardt, J. Klein, J.G. Richter, M. Vorländer: The ITA-Toolbox: An Open Source MATLAB Toolbox for Acoustic Measurements and Signal Processing, in 43th Annual German Congress on Acoustics, Kiel, Germany. 2017, pp. 222–225.
19. D.I. Blokhintzev: Acoustics of non-homogeneous moving media, NACA TM-1399, National Advisory Committee for Aeronautics. 1956.
20. R.G. Kouyoumjian, P.H. Pathak: A uniform geometrical theory of diffraction for an edge in a perfectly conducting surface. *Proceedings of the IEEE* 62, 11 (1974) 1448–1461.
21. International Organization for Standardization: ISO 9613–1:1993, Acoustics – Attenuation of sound during propagation outdoors – Part 1: Calculation of the absorption of sound by the atmosphere, 1993.
22. C. Dreier, M. Vorländer: Auralization of aircraft noise by means of numerical and analytical description of partial sound sources, in 46th Annual German Congress on Acoustics, Hannover, Germany. 2020, pp. 1145–1148.
23. K. Risse, E. Anton, T. Lammering, K. Franz, R. Hoernschemeyer: An integrated environment for preliminary aircraft design and optimization, in 53rd AIAA/ASME/ASCE/AHS/ASC Structures, Structural Dynamics and Materials Conference 20th AIAA/ASME/AHS Adaptive Structures Conference 14th AIAA, Honolulu, Hawaii, April 2012, American Institute of Aeronautics and Astronautics. 2012.
24. International Organization for Standardization: ISO 2533:1975, Standard Atmosphere. 1975.
25. R.O. Weber: Remarks on the definition and estimation of friction velocity. *Boundary-Layer Meteorology* 93, 2 (1999) 197–209.
26. ICAO: Doc 4444, Procedures for Air Navigation Services – Air Traffic Management, 16th ed. International Civil Aviation Organization, Montréal, Canada 2016.
27. J. Blauert: Spatial hearing: the psychophysics of human sound localization, Rev. ed edition, MIT Press, Cambridge, MA. 1997.
28. H. Fastl, E. Zwicker: Psychoacoustics: Facts and Models. Number 22 in Springer Series in Information Sciences, 3rd ed., Springer, Berlin; New York, 2007.
29. C. Dreier, M. Vorländer: Sound source modelling by nonnegative matrix factorization for virtual reality applications. *INTER-NOISE and NOISE-CON Congress and Conference Proceedings* 263, 5 (2021) 1053–1061.
30. German Institute for Standardization: DIN 45631:1991. Procedure for calculating loudness level and loudness. 1991.
31. German Institute for Standardization: DIN 45692:2009. Measurement technique for the simulation of the auditory sensation of sharpness. 2009.
32. F. Rietdijk: Auralisation of Airplanes Considering Sound Propagation in a Turbulent Atmosphere. PhD thesis, Chalmers University of Technology, Göteborg, Sweden, 2017.
33. R. Pieren, D. Lincke: Auralization of aircraft flyovers with turbulence-induced coherence loss in ground effect. *The Journal of the Acoustical Society of America* 151, 4 (2022) 2453–2460.
34. Institute for Hearing Technology and Acoustics: Virtual Acoustics – A real-time auralization framework for scientific research. 2021. <http://virtualacoustics.org/VA>.